Electronic Supplementary Material (ESI) for Chemical Communications


## Electronic Supporting Information

# β-(Ethynylbenzoic acid)-substituted push-pull porphyrins: DSSC dyes by a direct palladium-catalyzed alkynylation reaction.†

**Masatoshi Ishida,[a,b] Deasub Hwang,[a,c] Young Bean Koo,[a] Jooyoung Sung,[a] Dong Young Kim,[c] Jonathan, L. Sessler[a,d]* and Dongho Kim[a]***

[a] *Department of Chemistry, Yonsei University, Seoul 120-749, Korea*

[b] *Education Center for Global Leaders in Molecular Systems for Devices, Graduate School of Engineering, Fukuoka 819-0037, Japan*

[c] *Opto-electronic Materials Lab, Korea Institute of Science and Technology, Seoul, 136-791, Korea*

[d] *Department of Chemistry and Biochemistry, The University of Texas at Austin, Texas 78712-01224, United States*

**CORRESPONDING AUTHORS**

E-mail: dongho@yonsei.ac.kr (D. K)

E-mail: sessler@cm.utexas.edu (J. L. S)

**Instruments.** $^{1}$H-NMR (400 MHz) and $^{13}$C-NMR (100 MHz) spectra were recorded on a Bruker Avance II spectrometer. Chemical shifts ($\delta$-scale, ppm) were referenced to the residual solvent peaks (δ of 5.32 for proton and 53.8 for carbon for dichloromethane). MALDI-TOF mass spectra were recorded on a BRUKER microflex 2 LRF20 spectrometer using dithranol (1,8,9-trihydroxyantharacene) as a matrix. High-resolution mass spectra (HR-MS) were recorded on a JEOL JMS-700 FAB mass spectrometer with *m*-nitrobenzyl alcohol (NBA) as a matrix. Cyclic voltammetric measurements were carried out on a CHI 621D electrochemical analyzer using a conventional three-electrode cell for samples (1 mM) dissolved in dry THF containing 0.1 M $n$Bu$_4$NPF$_6$ (TBAPF$_6$) under an Ar atmosphere. A glassy carbon working electrode, a platinum wire counter electrode, and an Ag/Ag$^+$ reference electrode were used in all the experiments. The potentials were calibrated using the ferrocenium/ferrocene couple (+0.642 V vs NHE).

**Materials.** All reagents and solvents were obtained from highest grade commercial sources and used without further purification unless otherwise noted. Some chemicals (e.g., pyrrole (Alfa Aesar)) were purified by the distillation *in vacuo*. $H_2O$ was purified by distillation and filtration (Milli-Q). $TiCl_4$ (Fluka) was diluted with water to 2 M at 0 °C to make a stock solution, which was kept in a refrigerator and freshly diluted to 100 mM with water for each $TiCl_4$ treatment of the FTO-coated glass plates. $TiO_2$ paste (Ti-Nanoxide HT) was purchased from Solaronix. Analytical thin-layer chromatography (TLC) was performed on Merck silica gel 60 pre-coated aluminum sheets. Column chromatography was carried out using silica gel 60 (200 mesh, Merck). 5-Di-(*p-tert*-butylphenyl)amino-substituted-pinacolylborylated zinc(II) porphyrins (**1a** and **1b**) were prepared using previously reported procedures. [S1]

**Preparation of Mesoporous Anatase $TiO_2$ Nanospheres.** $TiO_2$ dispersions for use in an electrostatic spray process were prepared in accord with the method we reported previously.[S2] Briefly, to prepare modified mesoporous anatase $TiO_2$ spheres (UAM-015, Kotobuki), 0.3 mol of acetic acid was added dropwise to 0.3 mol of titanium isopropoxide with stirring at room temperature. The modified precursor that resulted was stirred for about 30 min and poured into 400 mL water as fast as possible with vigorous stirring. A white precipitate was formed instantaneously. Stirring was continued for an additional hour to allow the hydrolysis reaction to go to completion. After adding 6.2 mL of 65% aqueous nitric acid, the mixture was heated from room temperature to 80 °C over the course of 60 min and peptized for 2 h. The resultant mixture was kept in a titanium autoclave and heated at 250 °C for 12 h.

The dispersed $TiO_2$ solutions generated as per the above protocol were loaded into a plastic syringe that was connected to a high voltage power supply (BERTAN SERIES 205B). The

dispersed $TiO_2$ solutions were then electrosprayed directly onto a conducting FTO substrate (10 cm × 10 cm). An electric field of 15 kV was applied between the metal orifice and the conducting substrate. A feed rate, controlled by a syringe pump, of 35-30 μL/min was used. In order to form a uniform thickness over a large area, the nozzle and the substrate were placed on a motion control system regulated by a microprocessor.

**Device Fabrication.** To prepare the DSSC working electrode, a fluorine doped $SnO_2$ (FTO) conducting glass substrate (TEC 8, Pilkington) was first washed in a detergent solution using a sonicator bath for 10 min and then rinsed with water and ethanol. The resulting washed FTO glass substrates were then coated with the mesoporous anatase $TiO_2$ spheres obtained via electro-spray. Electrodes coated with $TiO_2$ were then annealed at 500 °C for 30 min. The film thickness of the annealed $TiO_2$ layer was measured and found to be 11~12 μm using an Alpha-step 200 surface profiler (Tencor P-10). A transparent $TiO_2$ film was prepared by using a commercial paste of highly transparent $TiO_2$ (Ti-Nanoxide HT, Solaronix). The working electrode was immersed into 0.1 M aqueous $TiCl_4$, a solution made up from an aqueous stock solution of 2 M $TiCl_4$ by appropriate dilutions. After treatment with $TiCl_4$, the $TiO_2$ films were washed with deionized water and ethanol, and then sintered at 500 °C for 30 min. After cooling to 80 °C, the working electrodes were immersed into solutions of the porphyrin dyes of this study (0.2 mM in ethanol) and allowed to stand overnight (15-20 h). To prepare the counter electrode, the FTO plates were drilled, and then washed first with deionized water and then 0.1 M HCl in ethanol with sonication for 10 min. After the FTO glass were washed in this way, the counter electrodes themselves were prepared by drop coating a solution of $H_2PtCl_6$ (0.5 mM in isopropyl alcohol) onto the FTO glass and then heating at 400 °C for 20 min.

The dye-adsorbed $TiO_2$ films and the platinum counter electrodes were assembled into sealed sandwich-type cells by heating with a hot-melt film (Surlyn 1702, 25 μm thickness, Dupont) used as a spacer between the electrodes. An aliquot of the electrolyte solution (0.22 M $[Co(bpy)_2]^{2+}$, 0.05 M $[Co(bpy)_3]^{3+}$, 0.1 M $LiClO_4$ and 0.5 M 4-*tert*-butylpyridine in acetonitrile) was then placed into a hole in the counter electrode of the assembled cells. The hole was sealed with a microscope cover glass and surlyn (25 μm thickness) to prevent leakage of the electrolyte solution.

**Steady-state Absorption and Fluorescence Measurement.** Steady-state absorption spectra in solution and on transparent $TiO_2$ were acquired using a UV-vis-NIR spectrometer (Varian, Cary5000). Steady-state fluorescence spectra were recorded on a fluorescence spectrometer (SCINCO, FS-2). The absorption spectra were corrected for contributions from the $TiO_2$ itself by subtracting the absorption of the bare $TiO_2$ layer.

**Picosecond Time-resolved Fluorescence Decay Measurement.** A time-correlated single-photon-counting (TCSPC) system was used for measurements of spontaneous fluorescence decay. As an excitation light source, a mode-locked Ti:sapphire laser (Spectra Physics, MaiTai BB) was used that provides ultrashort pulses (80 fs at full width half maximum, fwhm) with a high repetition rate (80 MHz). This high repetition rate may be slowed down to 1M ~ 800 kHz by using a homemade pulse-picker. The pulse-picked output pulse was frequency-doubled by a 1 mm thickness of a BBO crystal (EKSMA). The fluorescence was collected by a microchannel plate photomultiplier (MCP-PMT, Hamamatsu, R3809U-51) with a thermoelectric cooler (Hamamatsu, C4878) connected to a TCSPC board (Becker&Hickel SPC-130). The overall instrumental response function was about 25 ps (fwhm). A vertically polarized pump pulse by a Glan-laser polarizer was used to irradiate the samples, and a sheet polarizer, set at an angle complementary to the magic angle (54.7°), was placed in the fluorescence collection path to obtain polarization-independent fluorescence decays.

**Photovoltaic Properties Measurement.** The power conversion efficiencies (PCEs) of the DSSCs of this study were measured using a solar simulator (450 W, Oriel Co.) with an AM 1.5 global filter. The incident light intensity was adjusted with a NREL-calibrated Si solar cell (PV Measurements Inc.) to an intensity corresponding to 1 SUN (100 mW $cm^{-2}$). The tested solar cells were masked to an aperture area of ca. 0.25 $cm^2$. The photovoltaic characteristics of the DSSCs were obtained by applying an external potential bias to the cells and measuring the generated photocurrent with a Keithley model 2400 digital source meter. The voltage step and delay time of the photocurrent were 10 mV and 0.1 s, respectively. The incident photon-to-current efficiencies (IPCEs) were measured by using a potentiostat (Keithley 2400 source meter), a 300 W xenon lamp (Oriel Co.) in combination with a spectrapro-150 monochromator (Acton Research Co.), in the range of 400–800 nm. A cut-off filter of 400 nm was attached at the output slit of the monochromator to remove UV light. The light intensities were measured with a calibrated power meter (LM-2 VIS, Coherent) at each wavelength. Electrical impedance spectra (EIS) for DSSCs were measured with an impedance analyzer (Solatron 1260) at an open-circuit potential under AM1.5 full sun illumination, with frequencies of $10^{-1}$–$10^6$ Hz. The magnitude of the alternative signal was 10 mV. Impedance parameters were determined by fitting the impedance spectra using Z-view software.

**Density Functional Theory (DFT) Calculations.** Theoretical calculations were performed with the *Gaussian09* program suite using a supercomputer.[S3] All calculations were carried out using the density functional theory (DFT) method with Becke's three-parameter hybrid exchange functionals and the Lee-Yang-Parr correlation functional (B3LYP) employing the 6-31G(d) basis set for all atoms. [S4]

## Optimization of oxidative Sonogashira-type cross-coupling reaction of β-borylated porphyrins (1a) with terminal alkyne (2b)

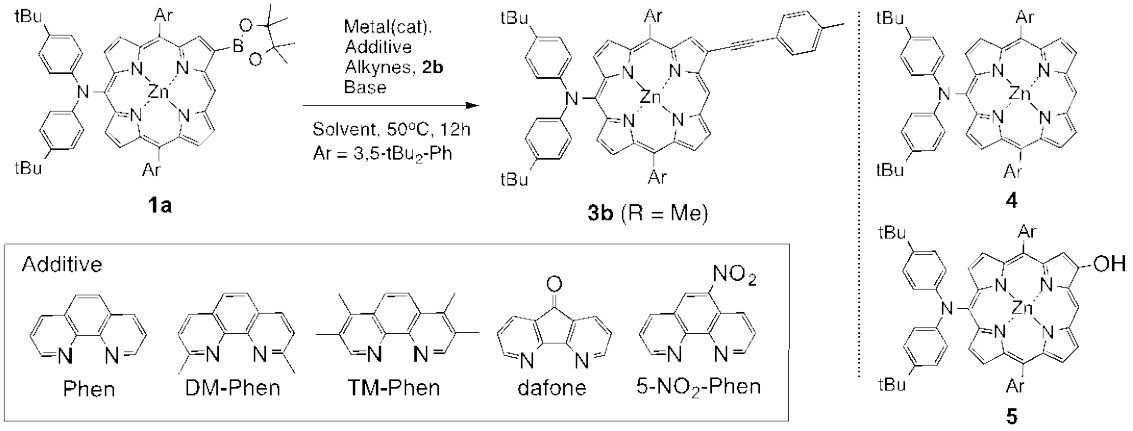


The reaction conditions for the coupling of monoborylated porphyrin **1a** with tolyacetylene (**2b**) were optimized by testing various organometallic catalytic conditions (see the following discussion and table). As noted in the text proper, a mild palladium-catalyzed oxidative coupling with 5-nitro-1,10-phenathroline as a supporting ligand in the presence of a base (e.g., NaH) under 1 atm of $O_2$ afforded the product in satisfactory yield.

The reported silver(I)-mediated Pd-catalyzed oxidative coupling conditions were unsuccessful in preparing **3b**, giving the β-hydroxy porphyrin (**5**) along with molecular degradation products (Entry 1 in the ensuing table). In the case of the cyclopalladated ferrocenylimine, no reaction was observed (Entry 2). In addition, the reported copper-catalysis condition did not afford good yields of the products (Entries 3-4). Using the palladium catalyst noted above and a DMF solvent system, the coupling reaction occurred in the presence of a stronger base such as NaH (Entry 5). Utilization of bidentated nitrogen ligands, which are known to be insensitive to air and moisture, improved the yield of the product. The 5-nitro-substituted 1,10-phenanthroline (5-$NO_2$Phen) was the most effective ligand and allowed the reaction to proceed smoothly (Entries 6-10). The reaction with the Pd-DM-Phen system was slow due to the steric hindrance around palladium active center (Entry 7). The choice of solvents and bases are likely critical (Entries 11-14). The reaction did not proceed without a palladium catalyst (Entry 15). Based on these findings, attempts were made to use a copper-Phen catalyst. While this did give some of the desired product of **3b**, unfortunately, the deborylated porphyrin (**4**) proved to be the major product (Entry 16). Therefore the palladium catalyst combination given as Entry 10 was chosen for ultimate use.

**Table S1.** Optimized conditions for the synthesis of **3b**[a]

| Entry | Metal(cat) | Additive | Solvent | Base | Yield[f] of 3b (%) |
|---|---|---|---|---|---|
| 1[b] | $Pd(dppf)Cl_2$ | $Ag_2O$ | $CH_2Cl_2$ | $K_2CO_3$ | trace |
| 2[c] | Palladcycle | $Ag_2O$ | $CH_2Cl_2$ | KOAc | n.d. |
| 3[d] | CuI | $Ag_2O$ | $C_2H_4Cl_2$ | $Cs_2CO_3$ | >10 |
| 4[e] | CuBr | - | MeOH | 2,6-lutidine | n.d. |
| 5 | $Pd(OAc)_2$ | - | DMF | NaH | 40 |
| 6 | $Pd(OAc)_2$ | Phen | DMF | NaH | 65 |
| 7 | $Pd(OAc)_2$ | DM−Phen | DMF | NaH | <21 |
| 8 | $Pd(OAc)_2$ | dafone | DMF | NaH | 45 |
| 9 | $Pd(OAc)_2$ | TM-Phen | DMF | NaH | 53 |
| 10 | $Pd(OAc)_2$ | 5-$NO_2$phen | DMF | NaH | 76 |
| 11 | $Pd(OAc)_2$ | 5-$NO_2$phen | $C_2H_4Cl_2$ | NaH | n.d. |
| 12 | $Pd(OAc)_2$ | 5-$NO_2$phen | DMSO | NaH | n.d. |
| 13 | $Pd(OAc)_2$ | 5-$NO_2$phen | DMF | $KO^tBu$ | 62 |
| 14 | $Pa(OAc)_2$ | 5-$NO_2$Phen | DMF | $K_2CO_3$ | 44 |
| 15 | - | 5-$NO_2$Phen | DMF | NaH | n.d. |
| 16 | CuI | 5-$NO_2$Phen | DMF | NaH | 34 |

[a]Reaction condtions; **1a** (25 μmol), **2b** (0.5 mmol), catalyst (7.5 μmol), additive (2 equiv. for Ag cation and 10.2 umol for N2-ligand), and dry solvent (2 mL) for 24 h under 1 atm of $O_2$ gas atmosphere. [b]Ref. S5, [c] ref. S6, [d] ref S7. [e] ref S8. [f]Yield of isolated product.

**Optimized Procedure for the Synthesis of Porphyrins of General Structure 3**

A borylporphyrin **1** (24 mg, 25 μmol), $Pd(OAc)_2$ (1.7 mg, 7.5 μmol), 1,10-phenanthroline (2.3 mg, 10.2 μmol), NaH (12 mg, 0.5 mmol), and 1-ethynylarene (**2**, 0.5 mmol) were placed in a Schlenk flask. The reaction vial was sealed, evacuated and backfilled with oxygen (a few times). Then, dry DMF (2.0 mL) was added and the reaction stirred at 40~50 °C for 24 h. The reaction mixture was diluted with $CH_2Cl_2$ and passed through a short silica gel pad. After evaporation of the solvent, the product was separated by column chromatography over silica gel using a hexanes/$CH_2Cl_2$ mixture as the eluent. Recrystallization from $CH_2Cl_2$/methanol afforded pure product.

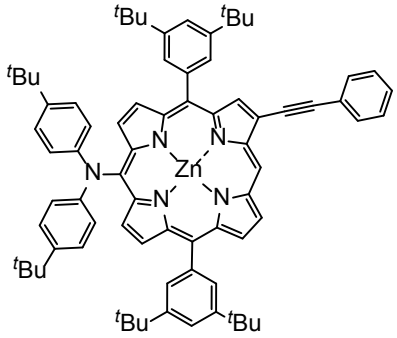


**3a** (R = H), Yield 67%, $^1$H NMR (400 MHz, $CD_2Cl_2$, 25 °C): $\delta$ = 10.51 (s, 1H, meso-H), 9.44 (d, $J$ = 4.5 Hz, 1H, β-H), 9.35 (d, $J$ = 4.5 Hz, 1H, β-H), 9.34 (d, $J$ = 4.5 Hz, 1H, β-H), 9.17 (s, 1H, β-H), 9.06 (d, $J$ = 4.5 Hz, 1H, β-H), 8.93 (d, $J$ = 4.5 Hz, 1H, β-H), 8.91 (d, $J$ = 4.5 Hz, 1H, β-H), 8.07 (d, J = 1.7 Hz, 2H, Ar-*o*-H), 8.06 (d, $J$ = 1.7 Hz, 2H, Ar-*o*-H), 7.97 (d, $J$ = 7.0 Hz, 2H, phenyl-H), 7.86 (t, $J$ = 1.7 Hz, 1H, Ar-*p*-H), 7.84 (t, $J$ = 1.7 Hz, 1H, Ar-*p*-H), 7.56 (t, $J$ = 7.0 Hz, 2H, phenyl-H), 7.50 (d, $J$ = 7.0 Hz, 1H, phenyl-H), 7.22 (d, $J$ = 9.4 Hz, 4H, N-Ar-H), 7.19 (d, $J$ = 9.4 Hz, 4H, *N*-Ar-H), 1.55 (s, 18H, *t*Bu-H), 1.54 (s, 18H, *t*Bu-H), 1.23 (s, 18H, *t*Bu-H); $^{13}$C NMR (100 MHz, $CD_2Cl_2$, 25 °C): $\delta$ = 153.20, 153.09, 151.80, 150.61, 150.51, 150.46, 150.16, 149.75, 149.25, 143.53, 141.56, 141.42, 135.08, 133.89, 133.58, 132.59, 132.22, 130.92, 130.75, 130.00, 129.69, 129.09, 126.22, 125.64, 124.01, 123.04, 122.75, 122.52, 121.78, 121.59, 104.34, 98.06, 85.32, 35.34, 34.35, 31.86, 31.51 ppm; FAB-MS: m/z = 1127.5802, Calcd for $C_{76}H_{81}N_5Zn$: 1127.5783 $[M]^+$; UV/vis ($CH_2Cl_2$): $\lambda_{max}$ = 421 and 563 nm.

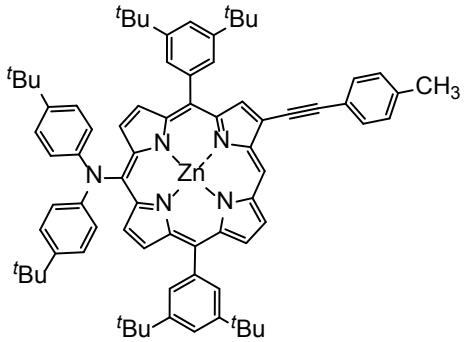


**3b** (R = Me), Yield 76%, $^1$H NMR (400 MHz, $CD_2Cl_2$, 25 °C): $\delta$ = 10.50 (s, 1H, meso-H), 9.43 (d, $J$ = 4.5 Hz, 1H, β-H), 9.35 (d, $J$ = 4.5 H, 1H, β-H), 9.34 (d, $J$ = 4.5 Hz, 1H, β-H), 9.13 (s, 1H, β-H), 9.04 (d, $J$ = 4.5 Hz, 1H, β-H), 8.92 (d, $J$ = 4.5 Hz, 1H, β-H), 8.90 (d, $J$ = 4.5 Hz, 1H, β-H), 8.06 (d, $J$ = 1.7 Hz, 2H, Ar-*o*-H),

8.05 (d, *J* = 1.7 Hz, 2H, Ar-*o*-H), 7.86 (t, *J* = 1.7 Hz, 2H, Ar-*p*-H), 7.85 (d, *J* = 7.9 Hz, 2H, tol-H), 7.37 (t, *J* = 7.9 Hz, 2H, tol-H), 7.22 (d, *J* = 9.4 Hz, 4H, *N*-Ar-H), 7.19 (d, *J* = 9.4 Hz, 4H, *N*-Ar-H), 2.48 (s, 3H, Me-H), 1.54 (s, 36H, *t*Bu-H), 1.23 (s, 18H, *t*Bu-H); $^{13}$C NMR (100 MHz, $CD_2Cl_2$, 25 °C): $\delta$ = 153.17, 153.07, 151.75, 150.57, 150.47, 150.18, 149.83, 149.71, 149.26, 143.55, 141.57, 141.44, 139.55, 134.82, 133.82, 132.52, 132.52, 132.09, 130.88, 130.74, 129.96, 129.82, 129.65, 126.20, 125.96, 123.06, 122.68, 122.52, 121.78, 121.58, 120.91, 104.33, 98.34, 84.64, 35.32, 34.33, 31.84, 31.49, 21.76 ppm; FAB-MS: m/z = 1141.5948. Calcd for $C_{77}H_{83}N_5Zn$: 1141.5940 $[M]^+$; UV/vis ($CH_2Cl_2$): $\lambda_{max}$ = 421 and 562 nm.

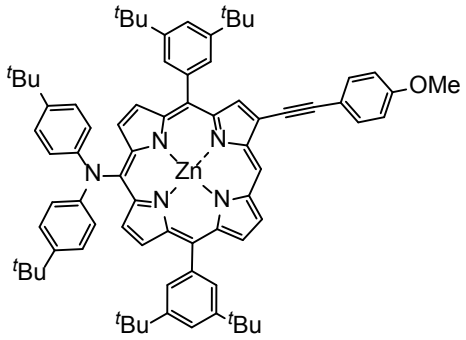


**3c** (R = OMe), Yield 72%, $^1$H NMR (400 MHz, $CD_2Cl_2$, 25 °C): $\delta$ = 10.40 (s, 1H, meso-H), 9.37 (d, *J* = 4.5 Hz, 1H, β-H), 9.29 (d, *J* = 4.5 Hz, 1H, β-H), 9.28 (d, *J* = 4.5 Hz, 1H, β-H), 9.06 (s, 1H, β-H), 8.99 (d, *J* = 4.5 Hz, 1H, β-H), 8.86 (d, *J* = 4.5 Hz, 1H, β-H), 8.84 (d, *J* = 4.5 Hz, 1H, β-H), 8.06 (d, *J* = 1.7 Hz, 2H, Ar-*o*-H), 8.05 (d, *J* = 1.7 Hz, 2H, Ar-*o*-H), 7.89 (d, *J* = 8.8 Hz, 2H, phenylene-H), 7.84 (t, *J* = 1.7 Hz, 1H, Ar-*p*-H), 7.83 (t, *J* = 1.7 Hz, 1H, Ar-*p*-H), 7.22 (d, *J* = 9.0 Hz, 4H, *N*-Ar-H), 7.18 (d, *J* = 9.0 Hz, 4H, *N*-Ar-H), 7.08 (d, *J* = 8.8 Hz, 2H, phenylene-H), 3.91 (s, 3H, Me-H), 1.54 (s, 18H, *t*Bu-H), 1.53 (s, 18H, *t*Bu-H), 1.23 (s, 18H, *t*Bu-H); $^{13}$C NMR (100 MHz, $CD_2Cl_2$, 25 °C): $\delta$ = 160.44, 152.99, 152.88, 151.58, 150.65, 150.36, 149.99, 149.64, 149.53, 149.07, 143.34, 142.05, 141.92, 134.41, 133.64, 133.49, 133.17, 132.22, 130.61, 130.48, 130.07, 129.76, 126.11, 125.76, 122.56, 122.18, 122.03, 121.72, 121.52, 121.31, 116.22, 114.68, 103.83, 97.74, 84.32, 54.34, 35.29, 34.30, 31.83, 31.47 ppm; FAB-MS: m/z = 1157.5885. Calcd for $C_{77}H_{83}N_5OZn$: 1157.5889 $[M]^+$; UV/vis ($CH_2Cl_2$): $\lambda_{max}$ = 421 and 563 nm.

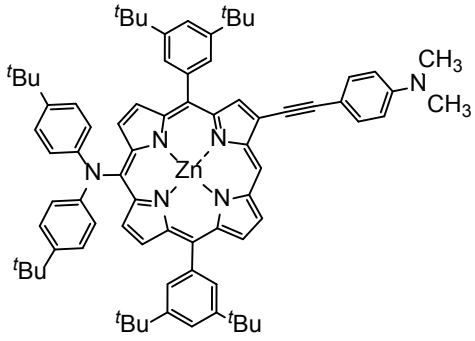


**3d** (R = $NMe_2$), Yield 84%, $^1$H NMR (400 MHz, $CD_2Cl_2$, 25 °C): $\delta$ = 10.40 (s, 1H, meso-H), 9.38 (d, *J* = 4.5 Hz, 1H, β-H), 9.28 (d, *J* = 4.5 Hz, 1H, β-H), 9.27 (d, *J* = 4.5 Hz, 1H, β-H), 9.00 (s, 1H, β-H), 8.98 (d, *J* = 4.5 Hz, 1H, β-H), 8.86 (d, *J* = 4.5 Hz, 1H, β-H), 8.83 (d, *J* = 4.5 Hz, 1H, β-H), 8.06 (d, *J* = 1.7 Hz, 2H, Ar-*o*-H), 8.05 (d, *J* = 1.7 Hz, 2H, Ar-*o*-H),

7.82-7.83 (m, 4H, Ar-*p*-H + phenylene-H), 7.22 (d, *J* = 9.0 Hz, 4H, *N*-Ar-H), 7.18 (d, *J* = 9.0, Hz, 4H, *N*-Ar-H), 6.85 (d, *J* = 8.8 Hz, 2H, phenylene-H), 3.06 (s, 6H, *N*-Me-H), 1.53 (s, 36H, *t*Bu-H), 1.23 (s, 18H, *t*Bu-H); $^{13}$C NMR (100 MHz, $CD_2Cl_2$, 25 °C): $\delta$ = 152.84, 152.75, 151.40, 150.91, 150.63, 150.34, 150.22, 150.01, 149.82, 149.03, 143.28, 142.08, 141.97, 133.70, 133.43, 133.27, 133.13, 132.16, 130.49, 130.43, 130.10, 129.74, 126.55, 126.11, 122.43, 122.02, 121.97, 121.67, 121.48, 121.28, 112.38, 110.52, 103.86, 99.32, 83.59, 40.44, 35.30, 34.31, 31.83, 31.48 ppm; FAB-MS: m/z = 1170.6254. Calcd for $C_{78}H_{86}N_6Zn$: 1170.6205 $[M]^+$; UV/vis ($CH_2Cl_2$): $\lambda_{max}$ = 414, 566 and 597 nm.

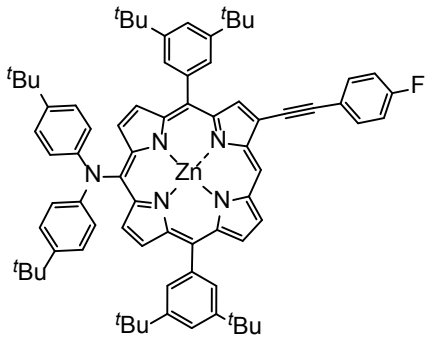


**3e** (R = F), Yield 54%, $^1$H NMR (400 MHz, $CD_2Cl_2$, 25 °C): $\delta$ = 10.47 (s, 1H, meso-H), 9.42 (d, *J* = 4.5 Hz, 1H, β-H), 9.35 (d, *J* = 4.5 Hz, 1H, β-H), 9.34 (d, *J* = 4.5 Hz, 1H, β-H), 9.15 (s, 1H, β-H), 9.04 (d, *J* = 4.5 Hz, 1H, β-H), 8.92 (d, *J* = 4.5 Hz, 1H, β-H), 8.90 (d, *J* = 4.5 Hz, 1H, β-H), 8.07 (d, J = 1.7 Hz, 2H, Ar-*o*-H), 8.06 (d, *J* = 1.7 Hz, 4H, Ar-*o*-H), 7.97 (d, *J* = 8.7 Hz, 2H, phenylene-H), 7.86 (t, *J* = 1.7 Hz, 1H, Ar-*p*-H), 7.85 (t, *J* = 1.7 Hz, 1H, Ar-*p*-H), 7.27 (t, *J* = 8.7 Hz, 2H, phenylene-H), 7.22 (d, *J* = 9.2 Hz, 4H, *N*-Ar-H), 7.19 (d, *J* = 9.2 Hz, 4H, *N*-Ar-H), 1.55 (s, 18H, *t*Bu-H), 1.54 (s, 18H, *t*Bu-H), 1.23 (s, 18H, *t*Bu-H); $^{13}$C NMR (100 MHz, $CD_2Cl_2$, 25 °C): $\delta$ = 163.40 (d, $J_{C\text{-}F}$ = 24.8 Hz), 153.42, 153.31, 152.00, 150.81, 150.67, 150.34, 149.85, 149.71, 143.73, 141.76, 141.63, 135.25, 134.42, 134.33, 134.03, 133.73, 132.70, 131.10, 130.93, 130.15, 129.87, 126.38, 125.60, 123.24, 121.91, 122.68, 121.97, 121.76, 116.59, 116.37, 104.40, 97.05, 85.25, 35.50, 34.51, 32.02, 31.67 ppm; FAB-MS: m/z = 1145.5652. Calcd for $C_{76}H_{80}N_5ZnF$: 1145.5689 $[M]^+$; UV/vis ($CH_2Cl_2$): $\lambda_{max}$ = 419 and 561 nm.

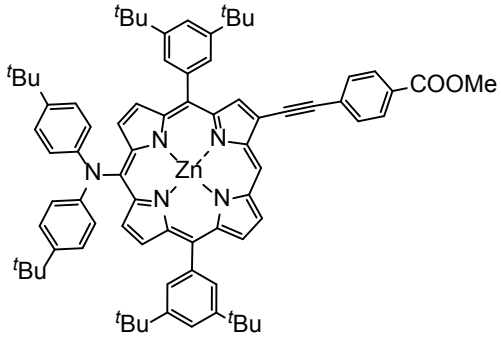


**3f** (R = COOMe), Yield 49%, $^1$H NMR (400 MHz, $CD_2Cl_2$, 25 °C): $\delta$ = 10.40 (s, 1H, meso-H), 9.36 (d, *J* = 4.5 Hz, 1H, β-H), 9.27 (d, *J* = 4.5 Hz, 1H, β-H), 9.25 (d, *J* = 4.5 Hz, 1H, β-H), 9.11 (s, 1H, β-H), 8.96 (d, *J* = 4.5 Hz, 1H, β-H), 8.83 (d, *J* = 4.5 Hz, 1H, β-H), 8.82 (d, *J* = 4.5 Hz, 1H, β-H), 8.07 (d, *J* = 8.3 Hz, 2H, phenylene-H), 7.98 (d, *J* = 1.7 Hz,

2H, Ar-*o*-H), 7.97 (d, *J* = 1.7 Hz, 2H, Ar-*o*-H), 7.94 (d, *J* = 8.3 Hz, 2H, phenylene-H), 7.78 (d, *J* = 1.7 Hz, 1H, Ar-*p*-H), 7.77 (d, *J* = 1.7 Hz, 1H, Ar-*p*-H), 7.13 (d, *J* = 9.0 Hz, 4H, *N*-Ar-H), 7.10 (d, *J* = 9.0 Hz, 4H, *N*-Ar-H), 3.85 (s, 3H, Me-H), 1.46 (s, 18H, *t*Bu-H), 1.45 (s, 18H, *t*Bu-H), 1.15 (s, 18H, *t*Bu-H); $^{13}$C NMR (100 MHz, $CD_2Cl_2$, 25 °C): $\delta$ = 166.96, 153.23, 153.09, 151.88, 150.62, 150.40, 149.95, 149.37, 149.12, 143.39, 141.94, 141.79, 135.40, 133.64, 133.32, 132.41, 132.07, 130.80, 130.56, 130.14, 130.07, 129.80, 128.92, 126.13, 124.45, 122.68, 122.56, 122.05, 121.75, 121.60, 121.36, 103.81, 96.83, 88.83, 52.58, 35.30, 34.31, 31.83, 31.47 ppm; FAB-MS: m/z = 1185.5828, Calcd for $C_{78}H_{83}N_5O_2Zn$: 1185.5838 $[M]^+$; UV/vis ($CH_2Cl_2$): $\lambda_{max}$ = 423 and 564 nm.

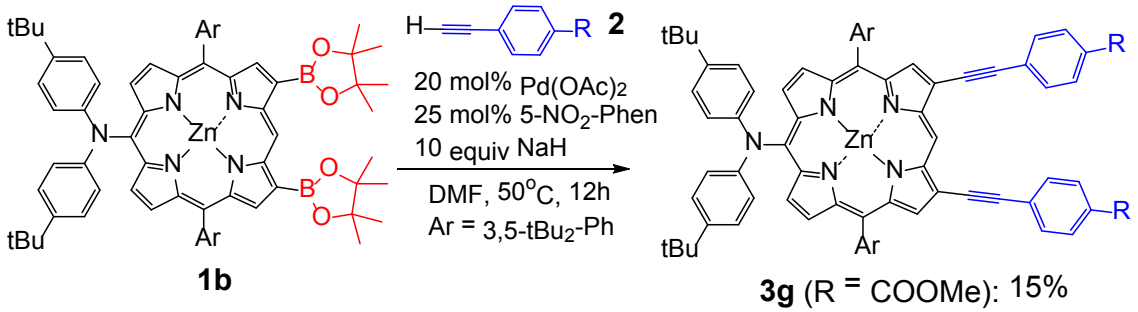


**3g** (R = COOMe), Yield 15% from **1b**; $^1$H-NMR (400 MHz) $\delta$ 10.76 (s, 1H, meso-H), 9.33 (d, *J* = 4.7 Hz, 2H, β-H), 9.14 (s, 2H, β-H), 8.89 (d, *J* = 4.7 Hz, 2H, β-H), 8.07 (d, *J* = 1.8 Hz, 4H, Ar-*o*-H), 7.90 (d, *J* = 8.3 Hz, 4H, phenylene-H), 7.88 (s, 2H, Ar-*p*-H), 7.76 (d, *J* = 8.3 Hz, 4H, phenylene-H), 7.23 (br s, 8H, *N*-Ar-H), 3.68 (s, 6H, Me-H), 1.52 (s, 36H, *t*Bu-H), 1.25 (s, 18H, *t*Bu-H) ppm. $^{13}$C NMR (100 MHz, $CD_2Cl_2$, 25 °C): $\delta$ = 166.31, 153.81, 150.69, 150.45, 150.16, 150.01, 149.34, 143.65, 141.24, 134.19, 131.86, 131.14, 129.68, 129.62, 128.34, 126.21, 125.49, 123.58, 123.10, 121.86, 97.73, 88.29, 35.32, 34.34, 31.84, 31.49 ppm; FAB-MS: m/z = 1343.6201, Calcd for $C_{88}H_{89}N_5O_4Zn$: 1343.6206 $[M]^+$; UV-Vis ($CH_2Cl_2$/nm); $\lambda_{max}$ = 436, 573 and 637.

**Hydrolysis of porphyrin esters.** The porphyrin methyl esters **3f** or **3g** (17 μmol) were dissolved in THF (2 mL). A solution of NaOH (2.0 M) dissolved in EtOH (3 mL) was then added. The resulting solution was stirred in an $N_2$ atmosphere at 70 ˚C for 24 h. The solvent was removed *in vacuo* to give a solid. Water, roughly 200 mL, was then added to give a colloidal suspension. A green solid (precipitate) was then obtained via the slow addition of 1.0 M HCl aq. to a final pH of 3. The solid was collected by filtration. The product was passed through a silica

gel column using a mixture of $CH_2Cl_2$/MeOH/AcOH (98:1.5:0.5) as the eluent. The pure product was obtained by recrystallization from a mixture of $CH_2Cl_2$/MeOH/$H_2O$.

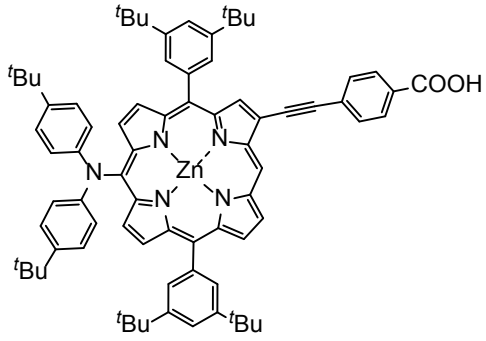


**ZnEP1**; Yield 88%, $^1$H NMR (400 MHz, $CD_2Cl_2$) δ 10.50 (s, 1H, meso-H), 9.45 (d, *J* = 4.6 Hz, 1H, *β*-H), 9.35 (d, *J* = 4.6 Hz, 1H, β-H), 9.34 (d, *J* = 4.6 Hz, 1H, *β*-H), 9.21 (s, 1H, *β*-H), 9.05 (d, *J* = 4.6 Hz, 1H, *β*-H), 8.92 (d, *J* = 4.6 Hz, 1H, β-H), 8.91 (d, *J* = 4.6 Hz, 1H, β-H), 8.25 (d, *J* = 8.4 Hz, 2H, *phenylene*-H), 8.05-8.08 (m, 6H, phenylene-H + Ar-*o*-H), 7.87 (t, *J* = 1.8 Hz, 1H, Ar-*p*-H), 7.85 (t, *J* = 1.8Hz, 1H, Ar-*p*-H), 7.20 (br s, 8H, *N*-Ar-H), 1.55 (s, 18H, *t*Bu-H), 1.54 (s, 18H, *t*Bu-H), 1.23 (s, 18H, *t*Bu-H); $^{13}$C NMR (100 MHz, $CD_2Cl_2$, 25 °C): *δ* = 178.77, 152.76, 152.65, 151.36, 150.17, 150.03, 149.72, 149.31, 149.16 148.82, 143.09, 141.12, 140.89, 134.65, 133.46, 133.14, 132.16, 131.78, 130.48, 130.32, 129.57, 129.26, 128.65, 125.79, 125.21, 123.58, 122.61, 122.32, 122.09, 121.34, 121.16, 103.90, 96.77, 88.57, 34.96, 33.97, 31.48, 31.12 ppm. FAB-MS: *m/z* = 1171.5690, calcd for $C_{77}H_{81}N_5O_2Zn$: 1171.5682 $[M]^+$; UV-Vis ($CH_2Cl_2$/nm); $\lambda_{max}$ = 422, 564, 592. Fluorescence ($CH_2Cl_2$/nm); $\lambda_{max}$ = 679.

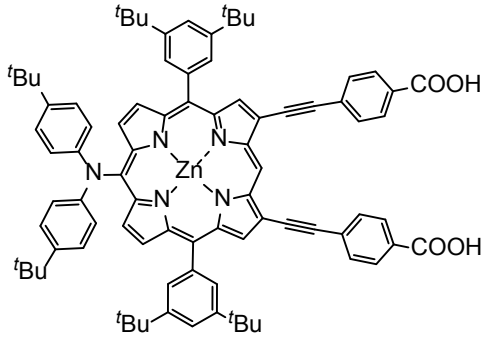


**ZnEP2:** Yield 76%, $^1$H NMR (400 MHz, $CD_2Cl_2$+$CD_3OD$) *δ* 10.67 (s, 1H, meso-H), 9.20 (d, *J* = 4.6 Hz, 2H, *β*-H), 9.05 (s, 2H, *β*-H), 8.76 (d, *J* = 4.6 Hz, 2H, β-H), 8.07 (d, *J* = 8.3 Hz, 4H, *phenylene*-H), 8.00 (d, *J* = 1.7 Hz, 4H, Ar-*o*-H), 7.90 (d, *J* = 8.3 Hz, 4H, *phenylene*-H), 7.81 (s, 2H, Ar-*p*-H), 7.18 (s, 8H, *N*-Ar-H), 1.51 (s, 36H, *t*Bu-H), 1.20 (s, 18H, *t*Bu-H) $^{13}$C NMR (100 MHz, $CD_2Cl_2$, 25 °C): *δ* = 153.41, 150.27, 149.65, 149.35, 148.77, 148.77, 143.02, 141.37, 134.60, 133.46, 131.56, 130.56, 129.95, 129.40, 125.74, 124.77, 122.27, 121.43, 121.20, 107.55, 96.87, 88.17, 34.86, 33.87, 31.34, 30.97 ppm. FAB-MS: *m/z* = 1315.5887; calcd for $C_{86}H_{85}N_5O_4Zn$: 1315.5893 $[M]^+$. UV-Vis ($CH_2Cl_2$/nm); $\lambda_{max}$ = 439, 573, 638. Fluorescence ($CH_2Cl_2$/nm); $\lambda_{max}$ = 697.

**Table S2.** Optical Properties and Electrochemical Data for Various Porphyrins and Driving Force for Electron Transfer Processes on $TiO_2$

| Compd | $\lambda_{abs}$/ nm[a] | *fwhm* / $cm^{-1}$[b] | $\lambda_{em}$/ nm[c] | $E_{0\text{-}0}$/ eV[d] | $\tau_{fl}$ / ns[c] | $E_{ox}$/ V[e] | $E_{red}$/ V[e] | $E_{ox}^*$/ V[f] | $\Delta G_{inj}$/ eV[g] | $\Delta G_{reg}$ / eV[h] |
|---|---|---|---|---|---|---|---|---|---|---|
| **ZnEP1** | 422(1.59)<br>564(0.16)<br>592(0.10) | 1455 | 679 | 1.91 | 1.46 | 0.94 | -0.83 | -0.97 | -0.47 | -0.40 |
| **ZnEP2** | 439(1.31)<br>573(0.15)<br>638(0.08) | 1517 | 697 | 1.85 | 1.35 | 0.98 | -0.78 | -0.87 | -0.37 | -0.42 |
| **YD1**[i] | 414(2.07)<br>587(0.1)<br>644(0.31) | 1708 | 672 | 1.88 | n.d. | 0.92 | -1.07 | -0.96 | -0.46 | -0.36 |

[a] Wavelengths for the absorption maxima in $CH_2Cl_2$ with extinction coefficients of samples, $\varepsilon$ ($\times 10^5$ $\cdot M^{-1} \cdot cm^{-1}$) shown in parentheses. [b]Full width at half maximum of B-bands. [c]Wavelengths for the reported emission maxima in $CH_2Cl_2$ were obtained by excitating at the B-band wavelength. [d] $E_{0\text{-}0}$ values were estimated from the intersection of the absorption and emission spectra. [e]First oxidation and reduction potentials determined by using cyclic voltammetry in THF containing 0.1 M *n*-$Bu_4NPF_6$ as a supporting electrolyte (vs. NHE). [f] Excited state oxidation potentials approximated from $E_{ox}$ and $E_{0\text{-}0}$ (vs. NHE). [g] Driving forces for electron injection from the porphyrin excited singlet state ($E_{ox}^*$) to the CB of $TiO_2$ (−0.5 V vs. NHE). [h] Driving force for regeneration of the porphyrin radical cation ($E_{ox}$) by reaction with the $Co(bpy)_3$ redox couple (+0.56 V vs NHE). [i]The values are reported in ref S9

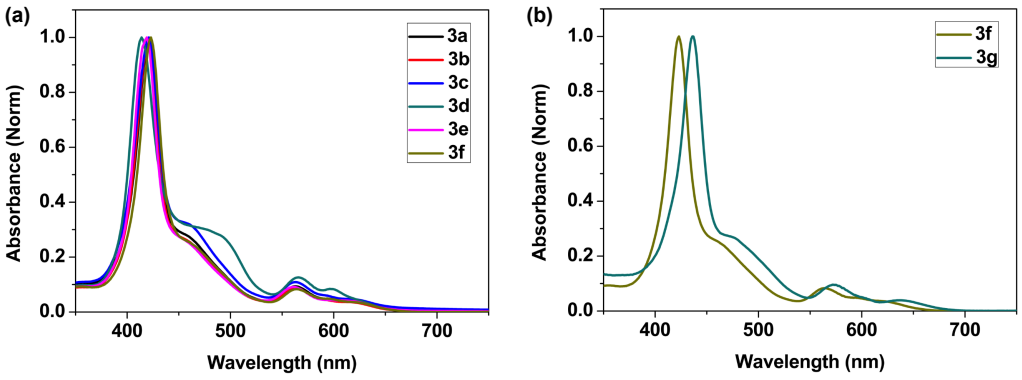


**Figure S1**. UV-vis absorption spectra of (a) singly-functionalized derivatives **3a-f** and (b) doubly-functionalized derivative, **3g** recorded in $CH_2Cl_2$.

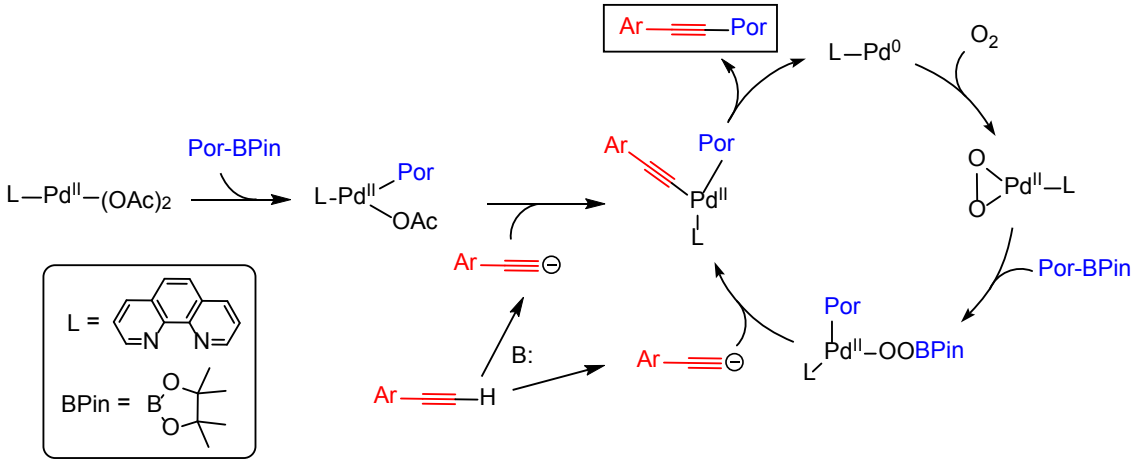


**Scheme S1.** Proposed mechanism for the cross-coupling reactions of borylated porphyrins and alkynes.

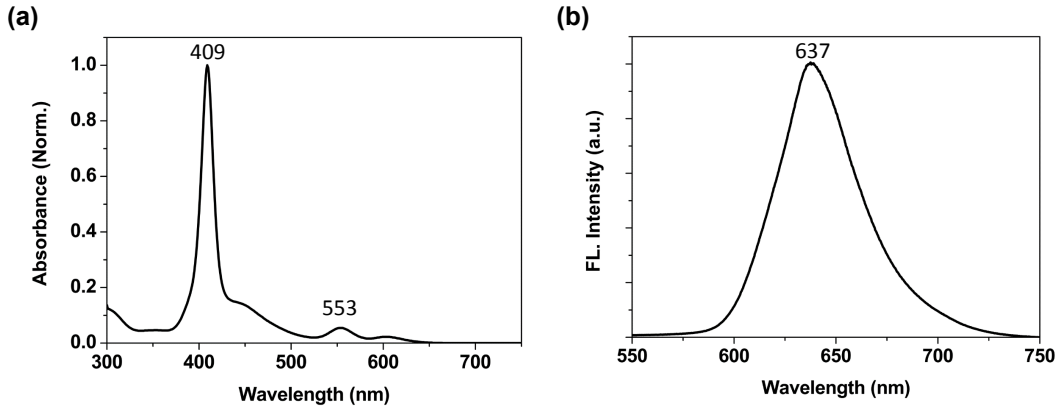


**Figure S2**. Steady-state (a) absorption and (b) emission spectra of β-unfunctionalized porphyrin (**4**) recorded in $CH_2Cl_2$ as a reference. The chemical structure of **4** is given in the catalyst optimization section above.

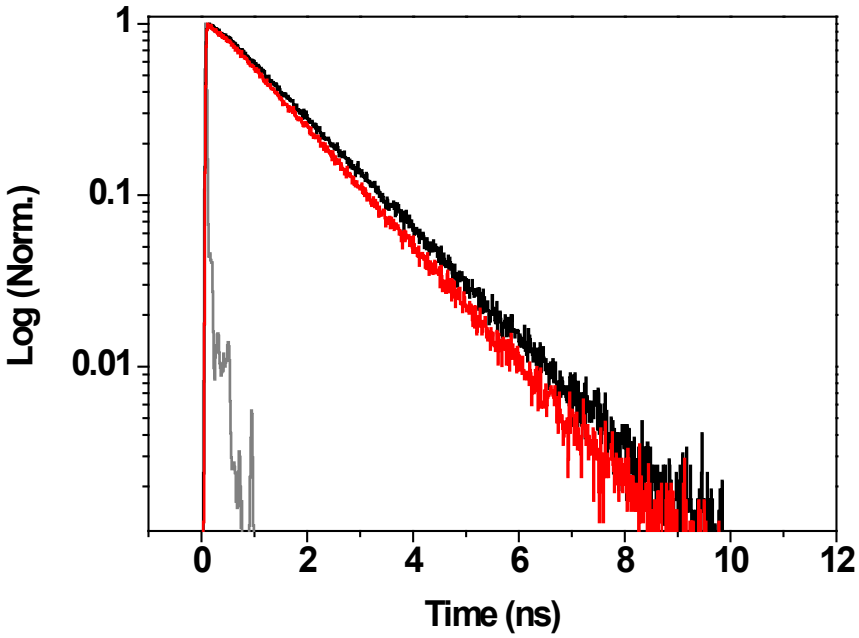


**Figure S3.** Time-resolved fluorescence decay profiles of **ZnEP1** (black line) and **ZnEP2** (red line) recorded in $CH_2Cl_2$ with photoexcitation effected at 400 nm. The temporal profile for the instrumental response function is plotted for comparison (grey line; fwhm of ~30 ps).

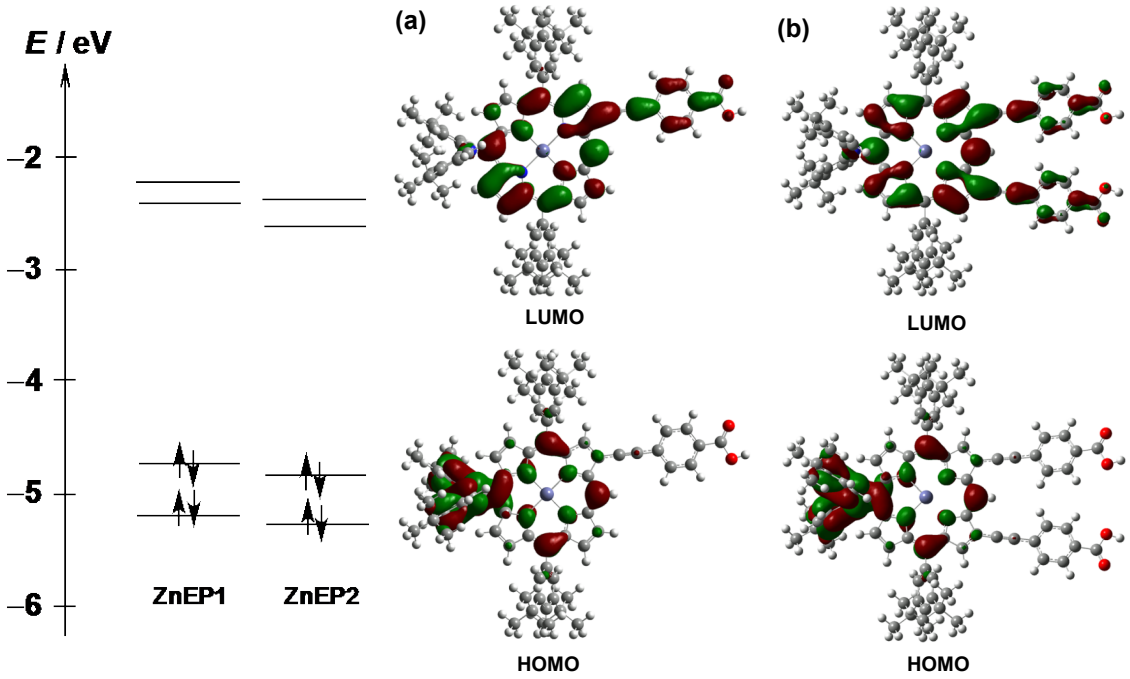


**Figure S4**. Molecular orbitals (HOMO and LUMO) and energy diagrams of (a) **ZnEP1** and (b) **ZnEP2** obtained from calculations carried out at the B3LYP/6-31G(d) level.

**Table S3.** Selected molecular orbital energy levels for porphyrins[a]

| | ZnEP1 | ZnEP2 | YD1[b] |
|---|---|---|---|
| LUMO+1 | -2.214 | -2.399 | -2.278 |
| LUMO | -2.422 | -2.585 | -2.578 |
| HOMO | -4.802 | -4.877 | -4.838 |
| HOMO-1 | -5.202 | -5.272 | -5.317 |

[a] Estimated by DFT calculations at the B3LYP/6-31G(d level). The energies are quoted in eV. [b] Ref S9.

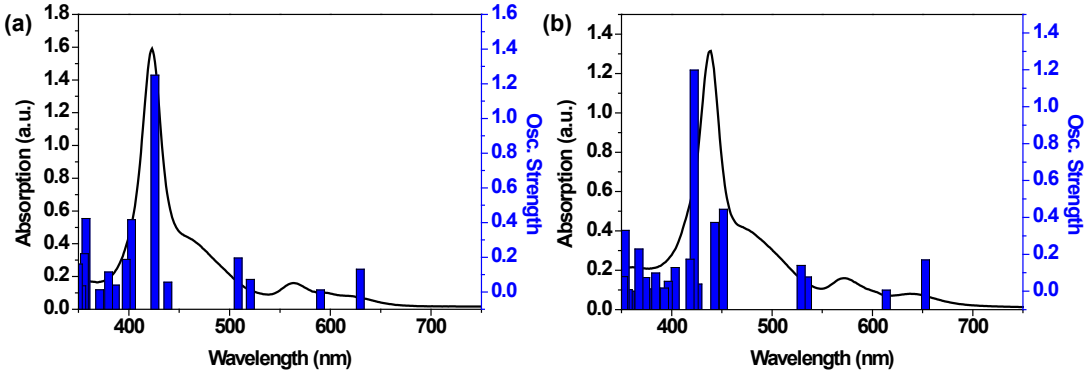


**Figure S5**. Simulated electronic states of (a) **ZnEP1** and (b) **ZnEP2** obtained using TD-DFT calculations carried out at the B3LYP/6-31G* level.

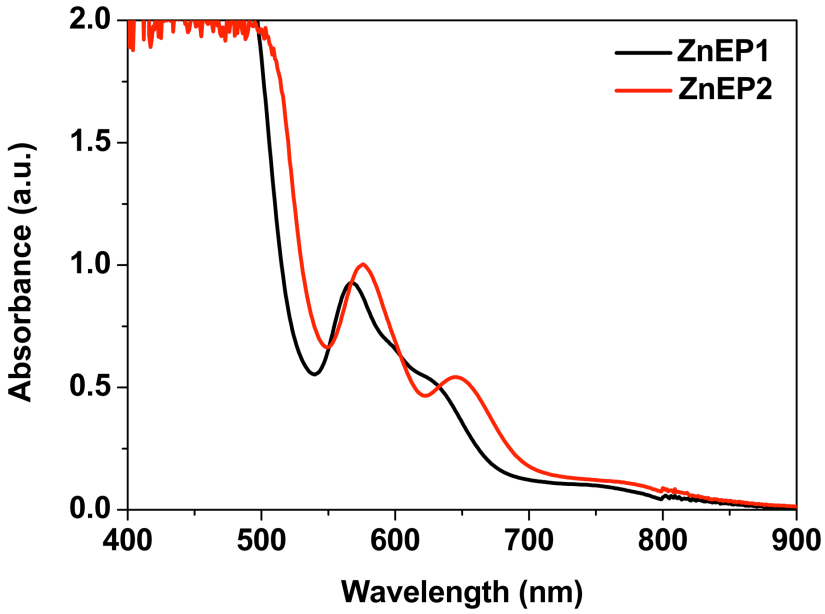


**Figure S6**. Absorption spectra of $TiO_2$ films modified with (a) **ZnEP1** and (b) **ZnEP2**, respectively. The weak broad bands (~700 nm) of the $TiO_2$/porphyrin electrodes may be attributed to the dye species. These spectral features have been reported in various D-π-A porphyrin dyes. See ref. S10.

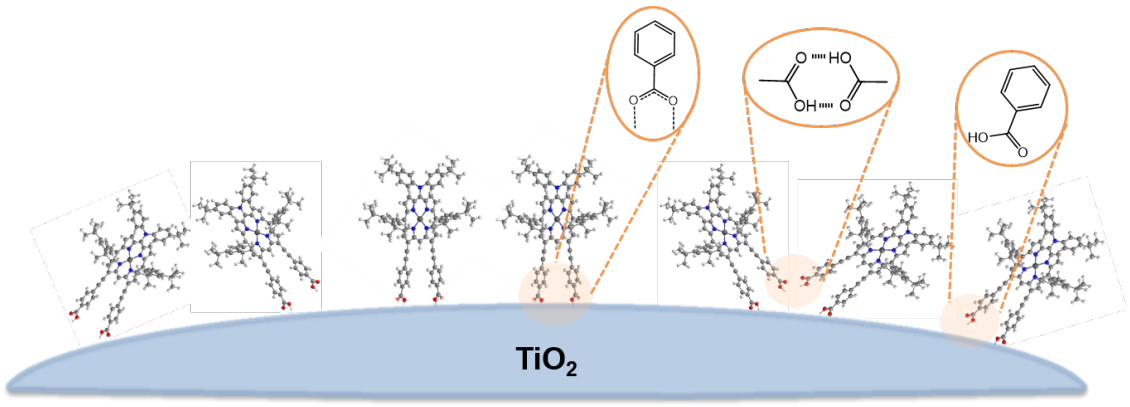


**Figure S7.** Schematic illustration of a possible geometry of the **ZnEP2** on $TiO_2$. The surface of $TiO_2$ is not fully covered by **ZnEP2** because of the unfavorable orientation (e.g., tilted geometry) of the dyes on the surface.

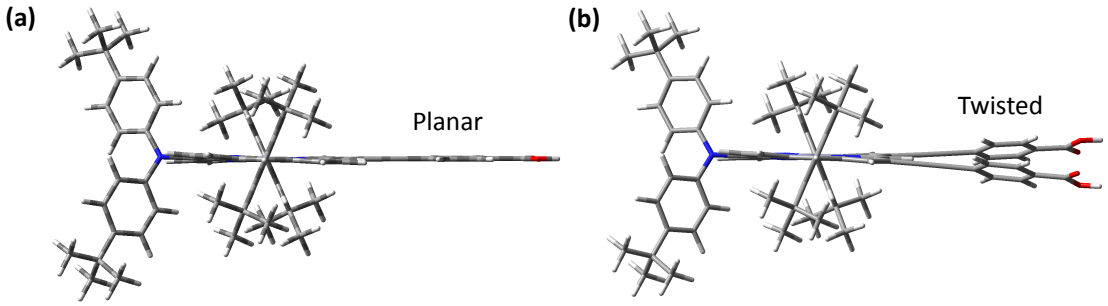


**Figure S8.** Side views of the optimized structures of (a) **ZnEP1** and (b) **ZnEP2**.

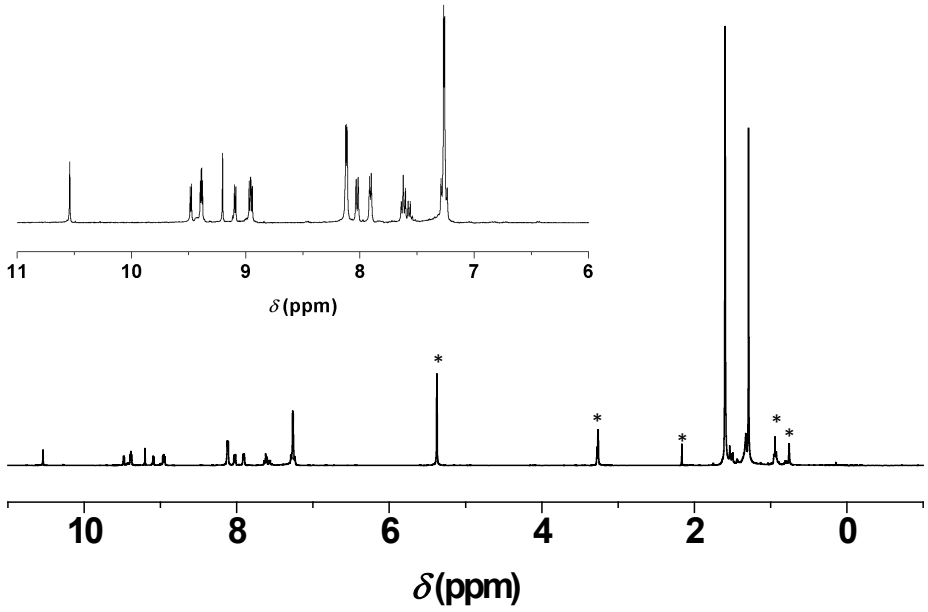


**Figure S9.** $^{1}$H NMR spectra of **3a** recorded in $CD_2Cl_2$. Inset shows the magnified aromatic region. Peaks marked with an asterisk arise from residual solvents and impurities.

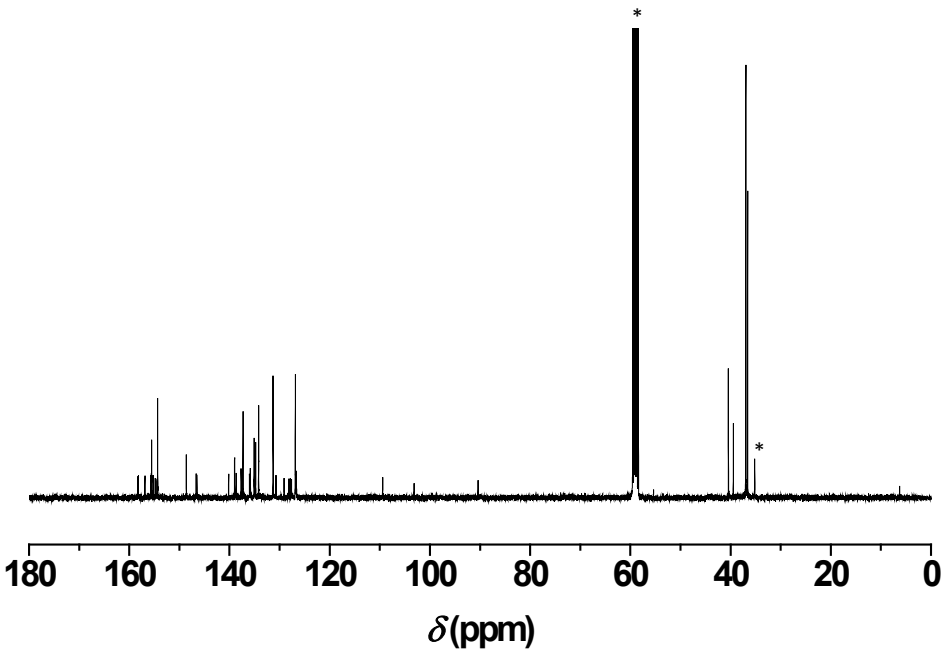


**Figure S10.** $^{13}$C NMR spectra of **3a** recorded in $CD_2Cl_2$. Peaks marked with an asterisk arise from residual solvents and impurities.

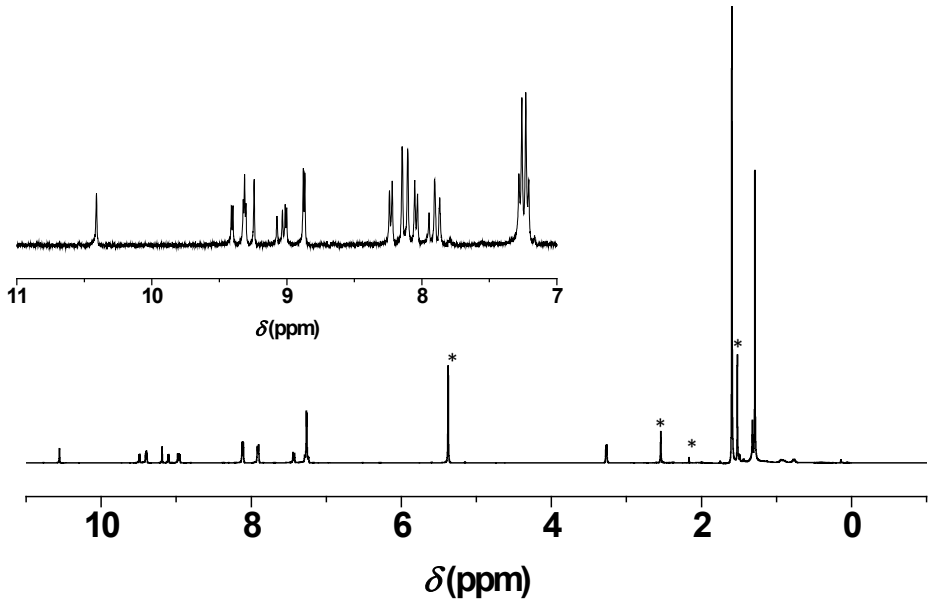


**Figure S11.** $^{1}$H NMR spectra of **3b** recorded in $CD_2Cl_2$. Inset shows the magnified aromatic region. Peaks marked with an asterisk arise from residual solvents and impurities.

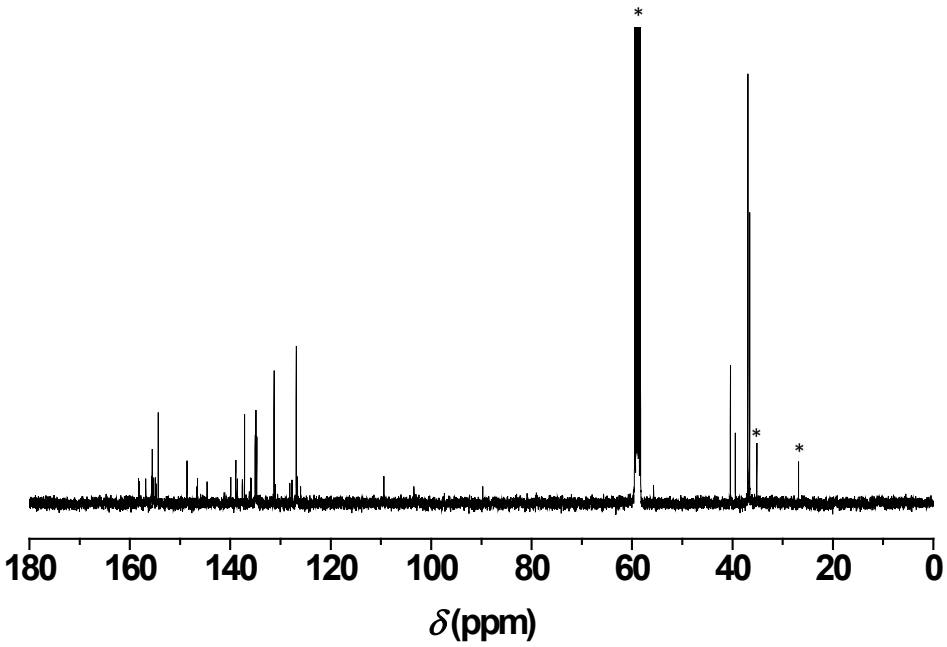


**Figure S12.** $^{13}$C NMR spectra of **3b** recorded in $CD_2Cl_2$. Peaks marked with an asterisk arise from residual solvents and impurities.

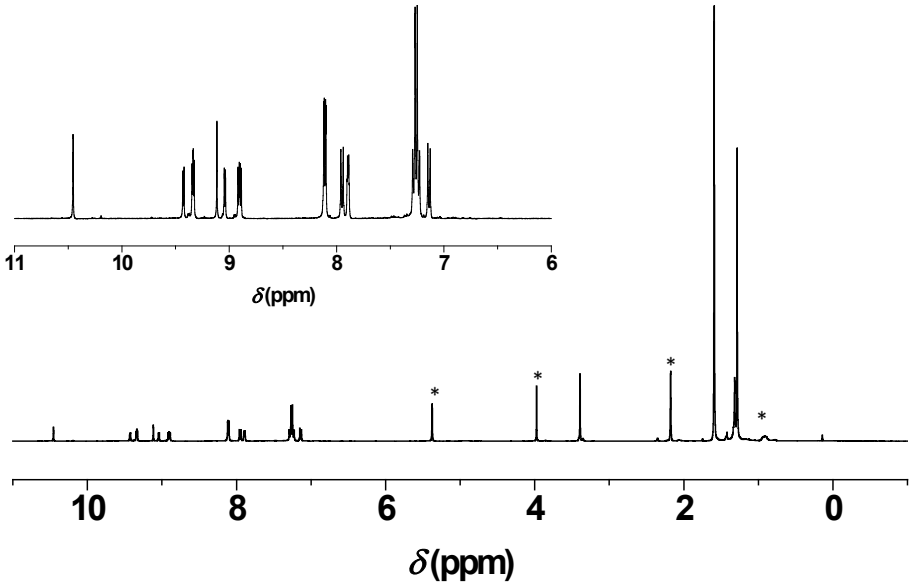


**Figure S13.** $^{1}$H NMR spectra of **3c** recorded in $CD_2Cl_2/CD_3OD$. Inset shows the magnified aromatic region. Peaks marked with an asterisk arise from residual solvents and impurities.

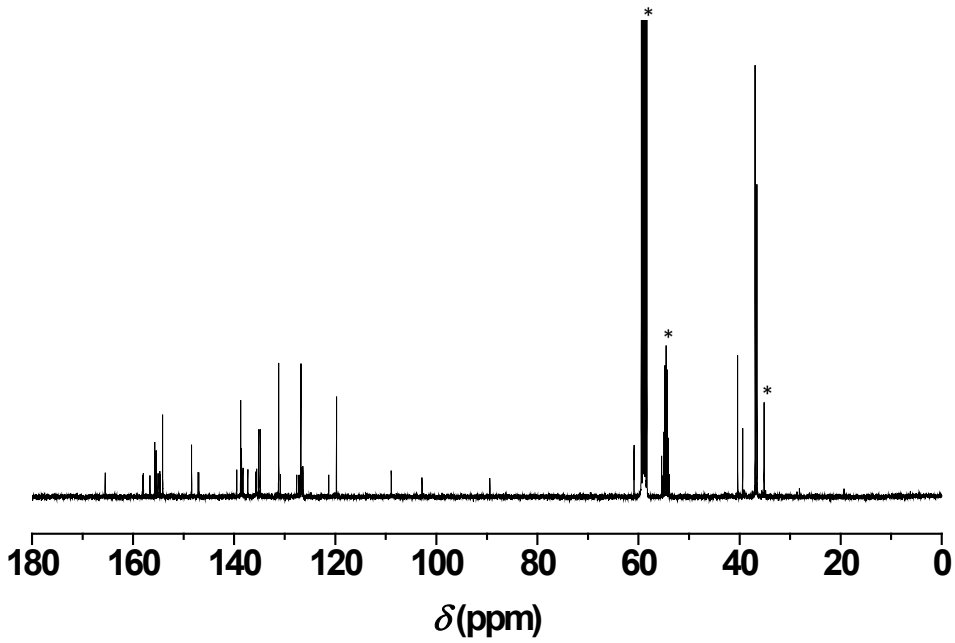


**Figure S14.** $^{13}$C NMR spectra of **3c** recorded in $CD_2Cl_2/CD_3OD$ Inset shows the magnified aromatic region. Peaks marked with an asterisk arise from residual solvents and impurities.

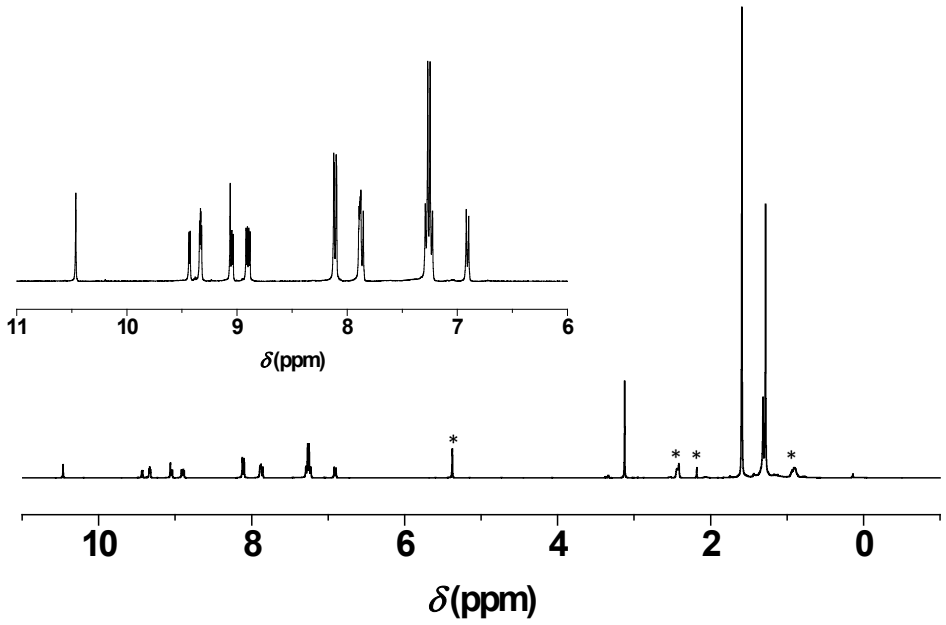


**Figure S15.** $^{1}$H NMR spectra of **3d** recorded in $CD_2Cl_2/CD_3OD$. Inset shows the magnified aromatic region. Peaks marked with an asterisk arise from residual solvents and impurities.

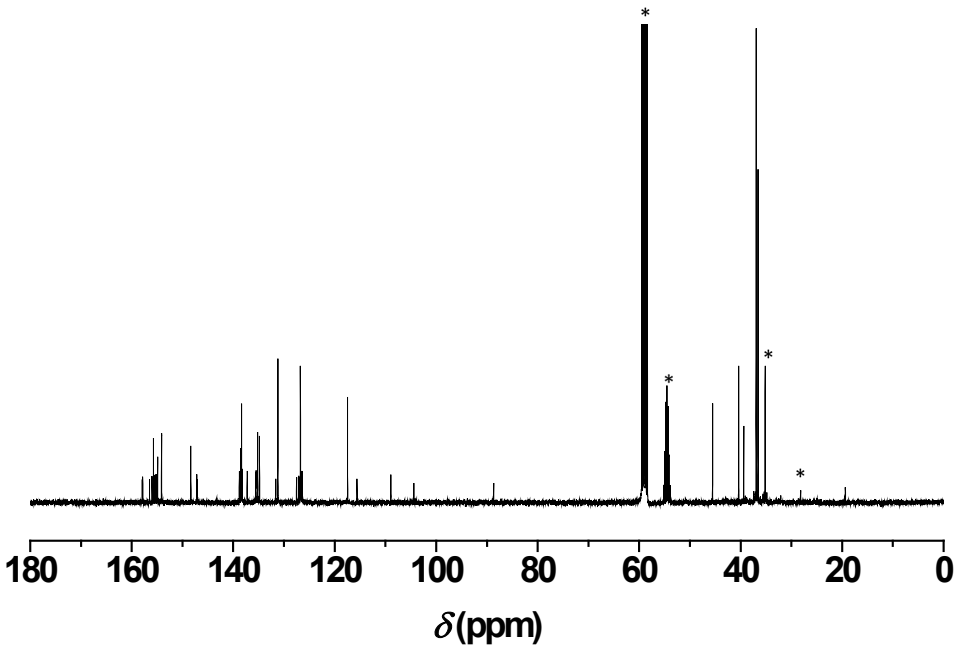


**Figure S16.** $^{13}$C NMR spectra of **3d** recorded in $CD_2Cl_2/CD_3OD$. Peaks marked with an asterisk arise from residual solvents and impurities.

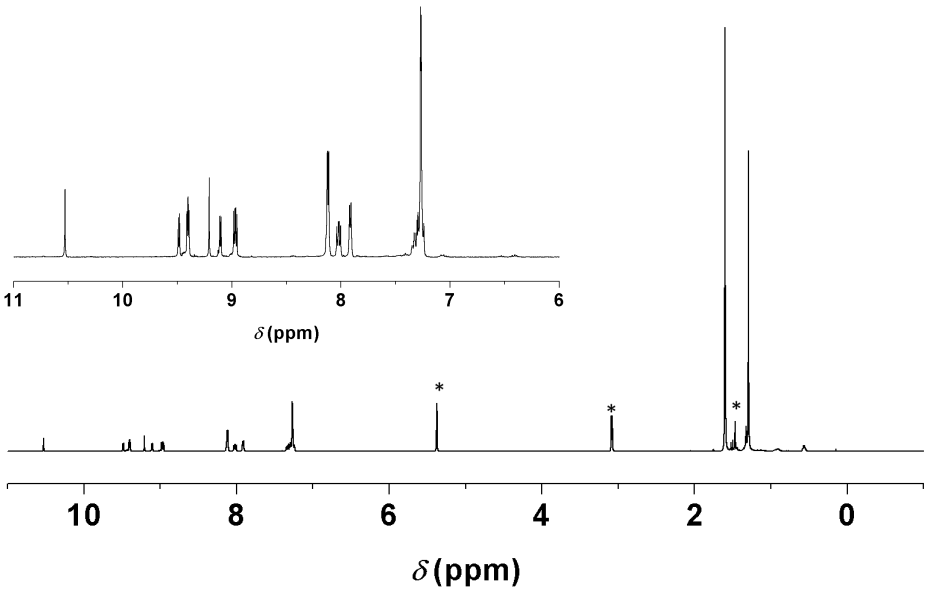


**Figure S17.** $^{1}$H NMR spectra of **3e** recorded in $CD_2Cl_2$. Inset shows the magnified aromatic region. Peaks marked with an asterisk arise from residual solvents and impurities.

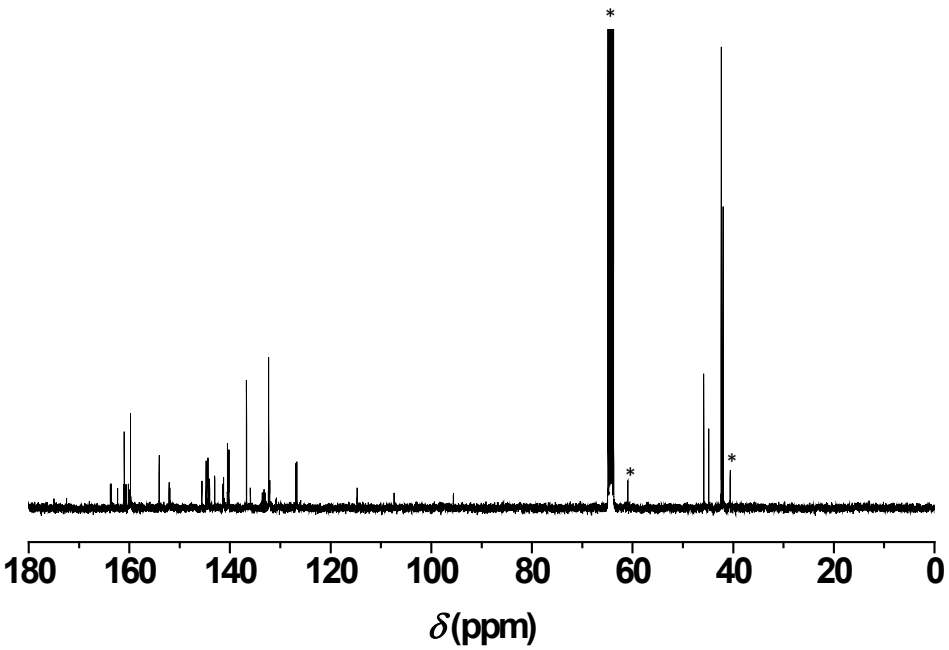


**Figure S18.** $^{13}$C NMR spectra of **3e** recorded in $CD_2Cl_2$. Peaks marked with an asterisk arise from residual solvents and impurities.

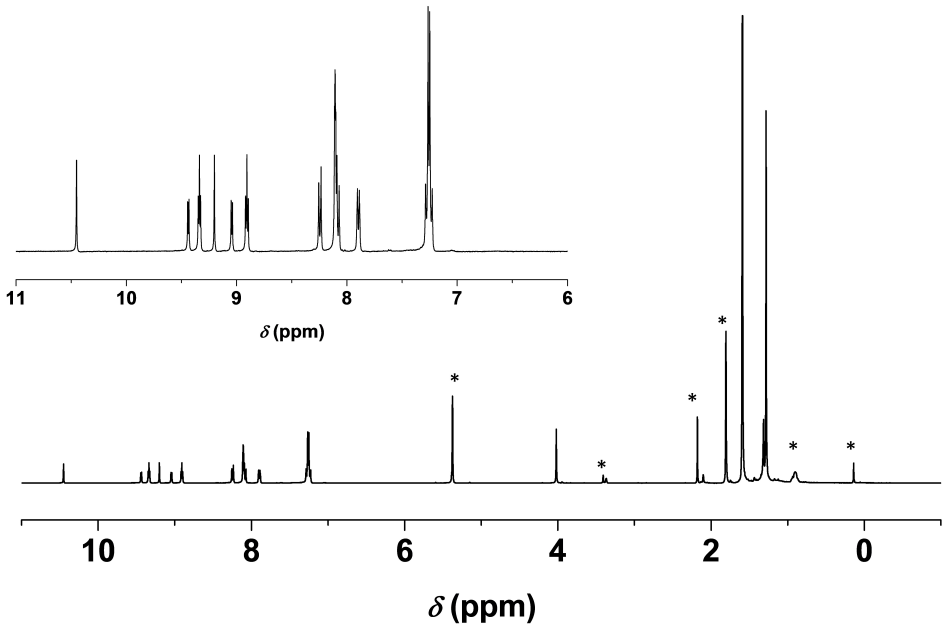


**Figure S19.** $^{1}$H NMR spectra of **3f** recorded in $CD_2Cl_2/CD_3OD$. Inset shows the magnified aromatic region. Peaks marked with an asterisk arise from residual solvents and impurities.

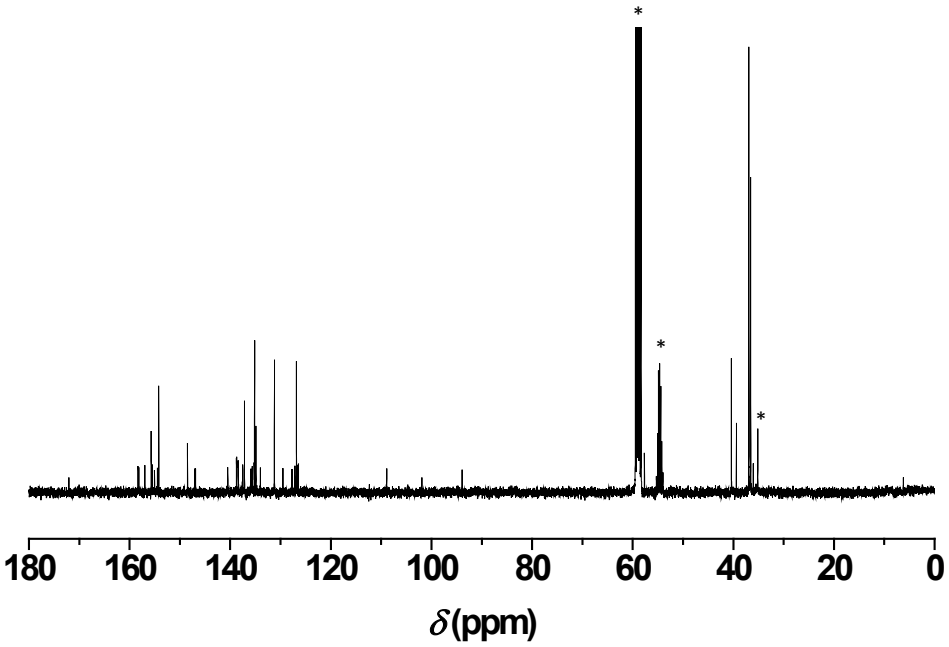


**Figure S20.** $^{13}$C NMR spectra of **3f** recorded in $CD_2Cl_2/CD_3OD$. Peaks marked with an asterisk arise from residual solvents and impurities.

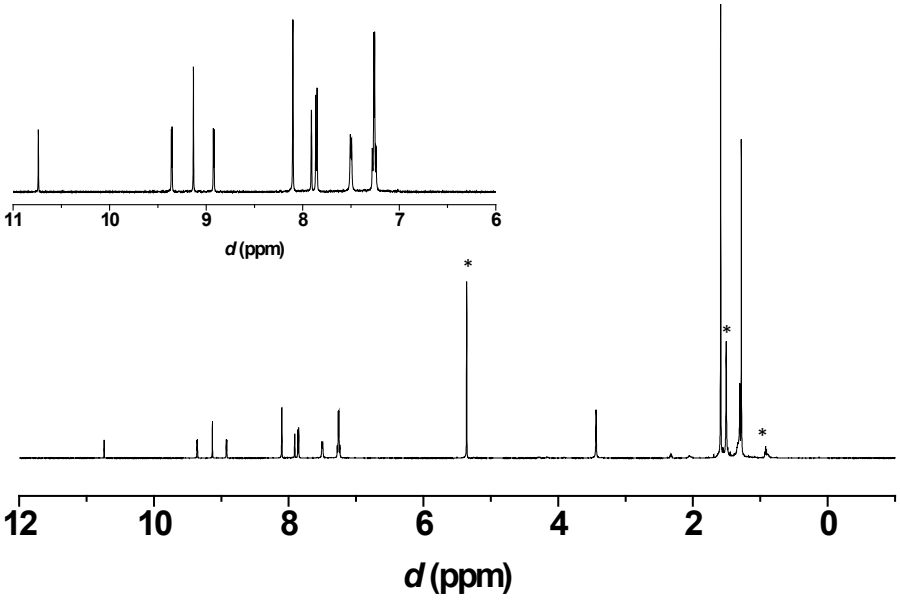


**Figure S21.** $^{1}$H NMR spectra of **3g** recorded in $CD_2Cl_2$. Inset shows the magnified aromatic region. Peaks marked with an asterisk arise from residual solvents and impurities.

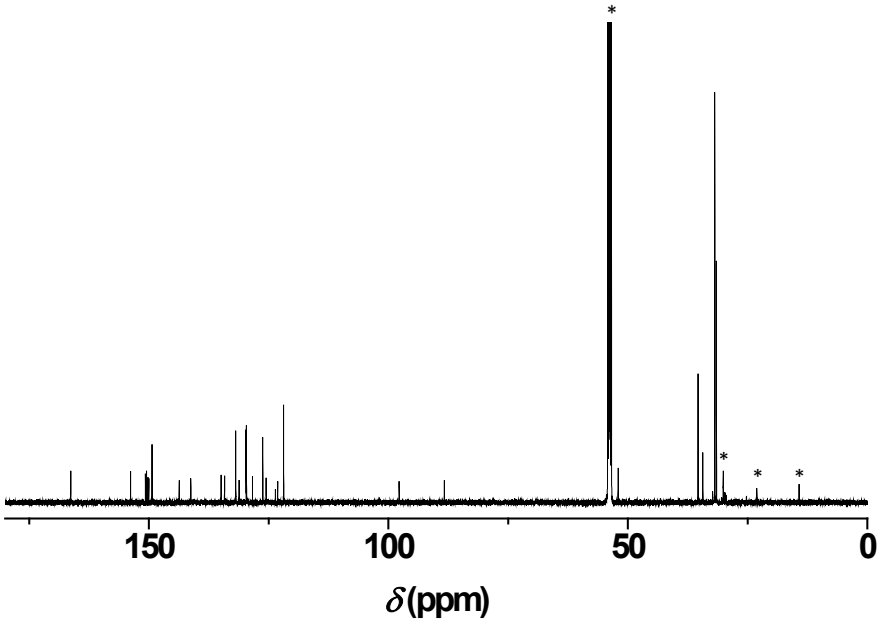


**Figure S22.** $^{13}$C NMR spectra of **3g** recorded in $CD_2Cl_2$. Peaks marked with an asterisk arise from residual solvents and impurities.

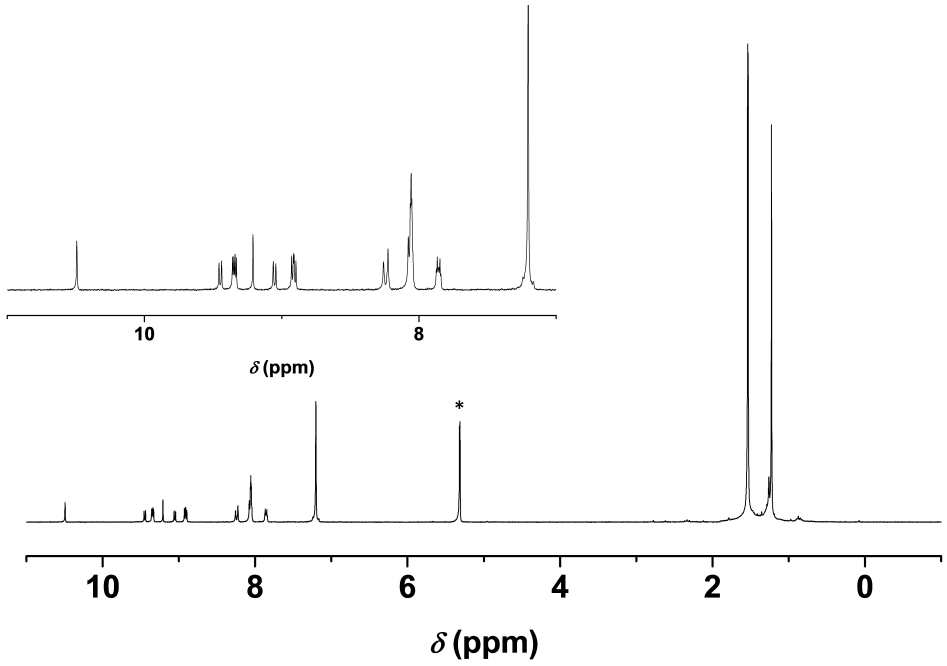


**Figure S23.** $^{1}$H NMR spectra of **ZnEP1** recorded in $CD_2Cl_2$. Inset shows the magnified aromatic region. Peaks marked with an asterisk arise from residual solvents and impurities.

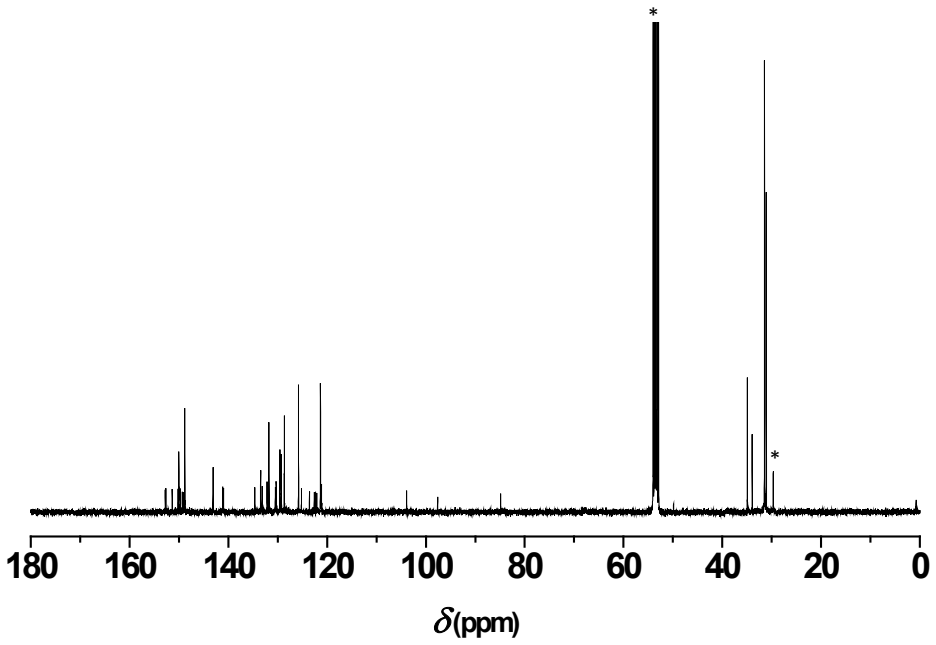


**Figure S24.** $^{13}$C NMR spectra of **ZnEP1** recorded in $CD_2Cl_2$. Peaks marked with an asterisk arise from residual solvents and impurities.

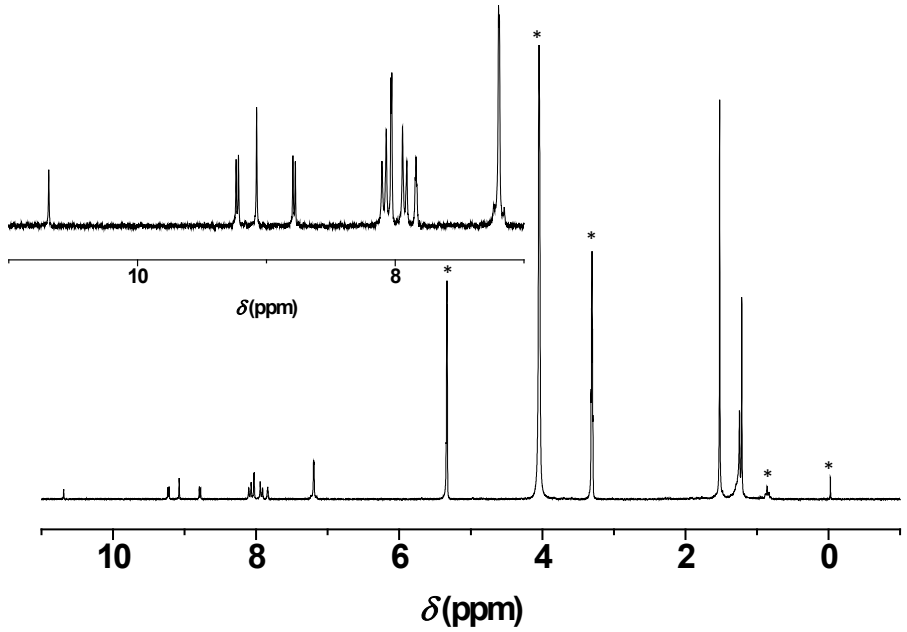


**Figure S25.** $^{1}$H NMR spectra of **ZnEP2** recorded in $CD_2Cl_2/CD_3OD$. Inset shows the magnified aromatic region. Peaks marked with an asterisk arise from residual solvents and impurities.

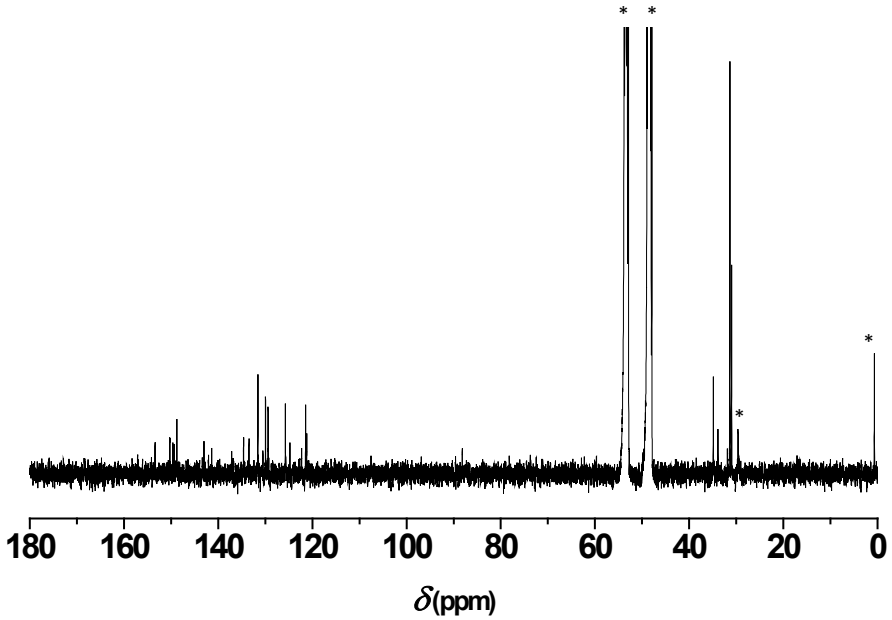


**Figure S26.** $^{13}$C NMR spectra of **ZnEP2** recorded in $CD_2Cl_2/CD_3OD$. Peaks marked with an asterisk arise from residual solvents and impurities.

**References**

S1) M. Ishida, S.W. Park, D. Hwang, Y. B. Koo, J. L. Sessler, D. Y. Kim and D. Kim, *J. Phys. Chem. C* 2011, **115**,19343.

S2) (a) D. Hwang, H. Lee, S. –Y. Jang, S. M. Jo, D. Kim, Y. Seo and D. Y. Kim, *ACS Appl. Mater. Interfaces* 2011, **3**, 2719; (b) D. Hwang, D. Y. Kim, S. –Y Jang and D. Kim, *J. Mater. Chem. A*, 2013, **1**, 1228.

S3) Gaussian 09, Revision A.1, M. J. Frisch, G. W. Trucks, H. B. Schlegel, G. E. Scuseria, M. A. Robb, J. R. Cheeseman, G. Scalmani, V. Barone, B. Mennucci, G. A. Petersson, H. Nakatsuji, M. Caricato, X. Li, H. P. Hratchian, A. F. Izmaylov, J. Bloino, G. Zheng, J. L. Sonnenberg, M. Hada, M. Ehara, K. Toyota, R. Fukuda, J. Hasegawa, M. Ishida, T. Nakajima, Y. Honda, O. Kitao, H. Nakai, T. Vreven, J. A. Montgomery, Jr., J. E. Peralta, F. Ogliaro, M. Bearpark, J. J. Heyd, E. Brothers, K. N. Kudin, V. N. Staroverov, R. Kobayashi, J. Normand, K. Raghavachari, A. Rendell, J. C. Burant, S. S. Iyengar, J. Tomasi, M. Cossi, N. Rega, N. J. Millam, M. Klene, J. E. Knox, J. B. Cross, V. Bakken, C. Adamo, J. Jaramillo, R. Gomperts, R. E. Stratmann, O. Yazyev, A. J. Austin, R. Cammi, C. Pomelli, J. W. Ochterski, R. L. Martin, K. Morokuma, V. G. Zakrzewski, G. A. Voth, P. Salvador, J. J. Dannenberg, S. Dapprich, A. D. Daniels, Ö. Farkas, J. B. Foresman, J. V. Ortiz, J. Cioslowski and D. J. Fox Gaussian, Inc., Wallingford CT, 2009.

S4) (*a*) A. D. Becke, *Phys. Rev. A,* 1988, **38**, 3098; (*b*) C. Lee, W. Yang and R. G. Parr, *Phys. Rev. B,* 1988, **37**, 785.

S5) G. Zou, J. Zhu and J. Tang, *Tetrahedron Lett*. 2003, **44**, 8709.

S6) F. Yang and Y. Wu, *Eur. J. Org. Chem*. 2007, 3476

S7) M. Wu, J. Mao, J. Guo and S. Ji, *Eur. J. Org. Chem*. 2008, 4050;

S8) T. Yasukawa, H. Miyamura and S. Kobayashi, *Org. Biomol. Chem.,* 2001, **9**, 6208.

S9) (a) C. –W. Lee, H. –P. Lu, C. –M. Lan, Y. –L. Huang, Y. –R. Liang, W. –N. Yen, Y. –C. Liu, Y. –S. Lin, E. W. –G. Diau and C. –Y. Yeh, *Chem. Eur. J.* 2009, **15**, 1403; (b) C. –P. Hsieh, H. –P. Lu, C. –L. Chiu, C. –W. Lee, S. –H. Chuang, C. –L. Mai, W. –N. Yen, S. –J. Hsu, E. W.-G. Diau and C. –Y. Yeh, *J. Mater. Chem*. 2010, **20**, 1127.

S10) S. Mathew, H. Iijima, Y. Toude, T. Umeyama, Y. Matano, S. Ito, N. V. Tkachenko, H. Lemmetyine and H. Imahori. *J. Phys. Chem. C.* 2011, **115**, 14415.